Appl Biol Chem (2017) 60(4):437–446
DOI 10.1007/s13765-017-0296-6

Online ISSN 2468-0842
Print ISSN 2468-0834

ARTICLE

Inactivation of the oxidase gene *mppG* results in the selective loss of orange azaphilone pigments in *Monascus purpureus*

Bijinu Balakrishnan[1] · Si-Hyung Park[2] · Hyung-Jin Kwon[1]

Received: 24 April 2017 / Accepted: 24 June 2017 / Published online: 29 June 2017

Abstract *Monascus* species are filamentous ascomycetes fungi and produce azaphilone (Az) pigment that is a well-known food colorant. Az is a class of fungal polyketides that bears a highly oxygenated pyranoquinone bicyclic core and is produced by a nonreducing fungal polyketide synthase with a reductive release domain (NR-fPKS-R). *MpPKS5* encodes an NR-fPKS-R for *Monascus* Az (MAz) and is clustered with four oxidoreductase genes including *mppG*; *mpp* designates *Monascus* pigment production. MAz pigments are classified as yellow and orange MAz, and their structures differ in two hydride reductions with yellow MAz as the reduced type. The biosynthesis of yellow MAz (monascin, **Y-1** and ankaflavin, **Y-2**) is completed by a reductive pathway involving a reductase gene *mppE*. This reductive pathway is diverged from a common MAz pathway involving two other reductase genes of *mppA* and *mppC*. This suggests that the biosynthesis of orange MAz (rubropunctatin, **O-1** and monascorubrin, **O-2**) is completed by an oxidative branch pathway and the cognate oxidative role of *mppG* is genetically characterized in the present study. A targeted gene inactivation mutant of Δ*mppG* displayed a severe impairment in the production of orange MAz with no significant alteration in the level of yellow MAz. The feeding experiment with **Y-1** in Δ*MpPKS5* indicated that **Y-1** could not be converted into **O-1**, which excludes the possibility that *mppG* mediates the conversion of yellow into orange MAz. This study supports the existence of divergent pathways in MAz biosynthesis and creates a recombinant strain for the selective production of yellow MAz.

Keywords Azaphilone pigment · *Monascus purpureus* · *mppG* · Oxidase gene · Selective production of monascin and ankaflavin

Introduction

Azaphilone (Az) consists of a group of fungal aromatic polyketides featuring the oxidized pyranoquinone bicyclic structure having a tertiary alcohol that is generally acylated. Az polyketides display diverse biological activities, which apparently involve interfering with specific protein–protein interactions [1]. The food fermentation fungus *Monascus* is well known for its high production of Az pigments, and *Monascus* ethanol extract has been used as a food colorant [2, 3]. The main pigment components of *Monascus* Az (MAz) are yellow (monascin, **Y-1** and ankaflavin, **Y-2**), orange (rubropunctatin, **O-1** and monascorubrin, **O-2**) and red MAz (rubropunctamine, **R-1** and monascorubramine, **R-2**) (Fig. 1). Yellow MAz contains a reduced pyranoquinone core and has a visible absorption peak at 390 nm. Orange MAz, bearing a typical Az pyranoquinone core, has a maximum absorption at 470 nm and is readily converted into red MAz in the presence of amine [4]. The color of orange MAz is pH sensitive, shifting to red and purple at pH values greater than 6.0 in aqueous ethanol [5]. The term Az was coined from the tendency of

✉ Hyung-Jin Kwon
hjink@mju.ac.kr

[1] Department of Biological Sciences and Bioinformatics, Myongji University, Yongin-si, Gyunggi-do 449-728, Republic of Korea

[2] Department of Oriental Medicine Resources and Institute for Traditional Korean Medicine Industry, Mokpo National University, Muan-gun, Jeollanam-do 534-729, Republic of Korea

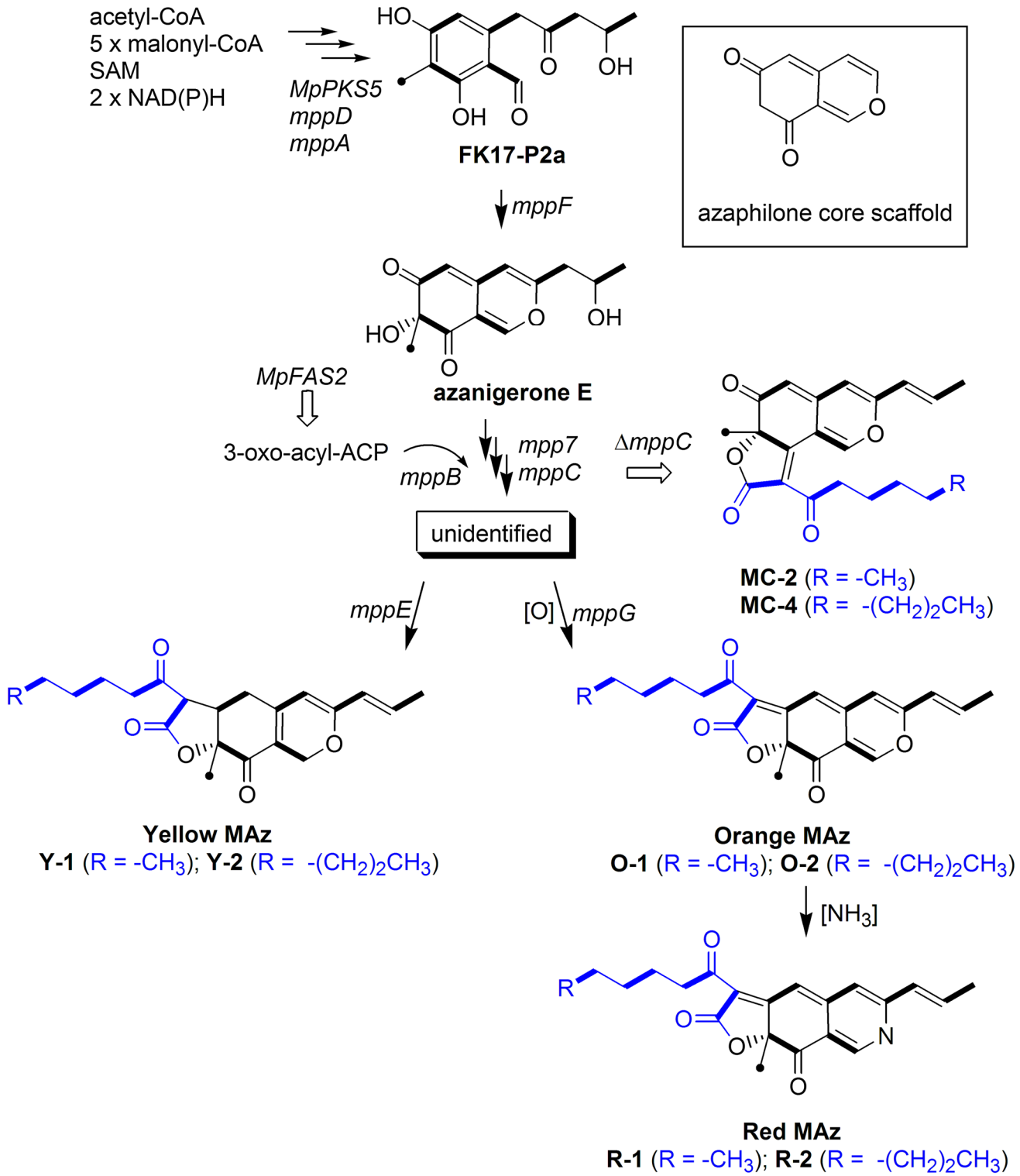

Fig. 1 Structures of MAz compounds with their proposed biosynthetic pathway, which is deduced by targeted gene inactivation studies [4, 24, 25, 27, 28]. The oxidative role of *mppG* in orange MAz production is demonstrated in this study. To emphasize the biosynthetic origin, the acetate units and *S*-adenosyl-L-methionine-derived carbons are denoted with bars and black dots, respectively. The compound names are in bold

incorporating nitrogen atom to generate a vinylogous γ-pyridone moiety, as exemplified in red MAz. It is thus not surprising to find diverse amino acid derivatives of red MAz in some *Monascus* culture extracts [6]. Many Az members, including yellow MAz, have no affinity for nitrogen, however. The MAz is not unique to *Monascus*, but it can also be found in other related filamentous fungi [7].

The health benefits of *Monascus*-fermented products are generally attributed to monacolin K (lovastatin), a well-known polyketide compound used for treating hypercholesterolemia [8, 9]. Recent studies have demonstrated that yellow MAz is also effective in blood lipid control [10], modulating lipoprotein metabolism in a health-benefitting manner [11]. In addition, several notable biological activities have been reported for yellow MAz, including anti-atherosclerosis [12], anti-diabetic [13, 14], anti-inflammatory [15, 16] and anti-obesity activities [17]. These support the notion that yellow MAz contributes to the health benefits associated with *Monascus* fermentation products [18]. The culture methods for promoting yellow MAz production have been developed. A high level of yellow MAz was obtained via a pH-static batch fermentation in a defined medium [19]. Nonionic surfactant-extractive fermentation afforded the accumulation of yellow MAz in culture supernatant with a high overall production [20]. An edible oil version of this method was also reported [21].

Biosynthetic genes for a microbial secondary metabolite are often clustered in chromosome, and their overall nucleotide sequence information provides an excellent opportunity for systematic study of the related biosynthetic mechanism [22, 23]. In an effort to delineate MAz biosynthetic pathway, we have identified MAz biosynthetic gene cluster from *Monascus pilosus* [4] and *M. purpureus* genome sequence [24] (Fig. 2A). The subsequent gene knockout studies in *M. purpureus* led us to consider a divergent pathway scenario for simultaneous production of yellow and orange MAz [24, 25]. All MAz compounds are produced from an aromatic polyketide pathway with nonreducing fungal polyketide synthase with a reductive release domain (NR-fPKS-R) [4, 26]. The MAz NR-fPKS-R (MpPKS5) pathway involves azanigerone E, which is further processed to be divergently converted into yellow or orange MAz (Fig. 1). The involvement of azanigerone E in MAz biosynthesis is supported by these two findings, the hydroxylation-mediated conversion of FK17-P2a into azanigerone E, demonstrated in azanigerone biosynthesis [26], and accumulation of FK17-P2a in *M. purpureus* knockout mutant of the hydroxylase gene *mppF* [25]. Azanigerone E is proposed to be decorated with a 3-oxo-acyl moiety that is generated by MpFAS2 with the assistance of the acyltransferase MppB in MAz biosynthesis [4, 27]. It is also proposed that the subsequent modifications by Mpp7 and MppC generate a hypothetical intermediate that then diverge into reductive (yellow MAz) and oxidative (orange MAz) pathways [24, 25] (Fig. 1).

It was previously shown that inactivation of *mppE* in *M. purpureus* resulted in a significant reduction in yellow MAz with a concomitant increase of orange MAz [28]. This indicated that *mppE* is involved in the biosynthesis of yellow MAz, implying a role for MppE in the reduction of the pyranoquinone core during yellow MAz biosynthesis (Fig. 1). The expression of an extra copy of *mppE* in *M. purpureus* failed to promote the production of yellow MAz in potato dextrose media but was effective in doing so in a chemically defined medium culture [28]. Considering the structural differences between yellow and orange MAz, we hypothesized that an oxidative modification is involved at a late stage of orange MAz biosynthesis. The MAz biosynthetic gene cluster encodes only one oxidase gene candidate, *mppG* (the gene model of CE4855_5133 and protein ID of 4856 in the *M. purpureus* genome sequence browser in the Joint Genome Institute portal) [24]. The *mppG* region was initially annotated in a part of *mppD* to encode an amine oxidase domain [4] and was lately annotated as a discrete oxidase gene [24] (Fig. 2A). MppG is predicted to be a flavin-containing oxidase and is not found in any other Az biosynthetic gene clusters so far reported.

In this study, we demonstrated that an *mppG* knockout mutant resulted in a dramatic reduction of orange MAz while retaining the production of yellow MAz. These findings support the divergent pathway proposal and provide a genetic engineering strategy for the preparation of yellow MAz with a minimal production of orange MAz.

Materials and methods

Strains, culture conditions and extraction methods

Monascus purpureus KACC (Korean Agricultural Culture Collection) 42430 and *Agrobacterium tumefaciens* AGL1 were used in this study. *M. purpureus* and its derivatives were maintained on potato dextrose agar (PDA) for 7 days at 30 °C [29]. The PDA volume in each plate was approximately 50 mL. Five pieces of 1 cm^3 agar blocks from the PDA culture were used to initiate a potato dextrose broth culture (PDB; Gellix™, Ventech Bio, Seoul, Republic of Korea). This PDB brand affords a high level of orange MAz production from the *M. purpureus* strain used in this study. The culture condition and pigment extraction method were previously described [28]. The organic extract from each 50 mL culture was dissolved in 1 mL methanol and was used in high-performance liquid chromatography (HPLC) analyses. For the feeding experiment

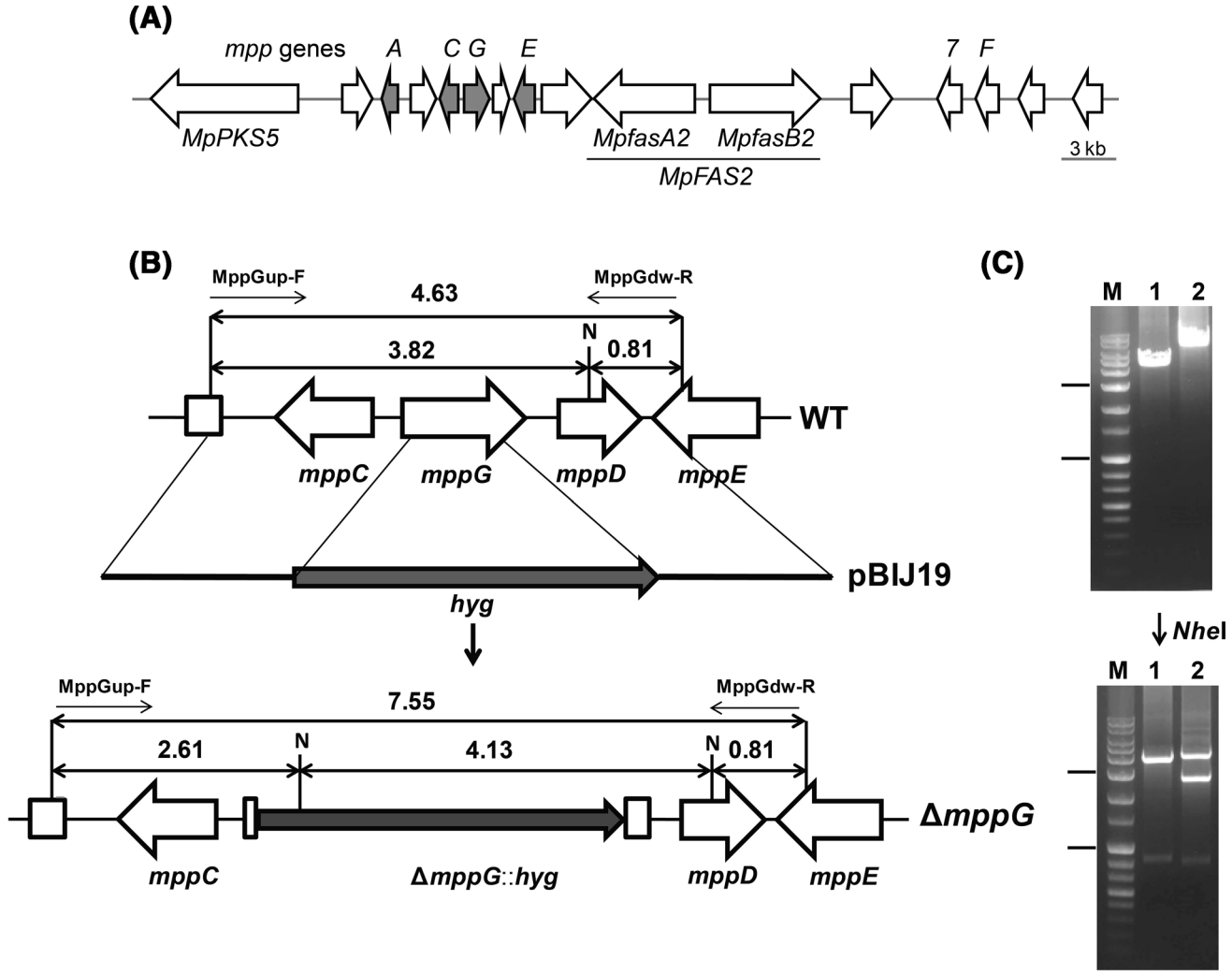

Fig. 2 Gene inactivation of *mppG* in *M. purpureus.* (**A**) Genetic organization of MAz biosynthetic gene cluster in *M. purpureus*. *MpPKS5* encodes NR-fPKS-R for MAz biosynthesis [4]. The products of *MpFasA2* and *MpFasB2* are deduced to constitute a fatty acid synthase MpFAS2, which generates short-chain oxo-acyl moieties for MAz production [27]. Four oxidoreductase genes are highlighted with filled arrows. (**B**) A *Nhe*I restriction map of the DNA region flanking *mppG* in WT, pBIJ19 and the resulting Δ*mppG* mutant. The size of each DNA fragment is shown in kb above the corresponding arrow. (**C**) Analytical PCR results of total DNA from the WT strain (*lane 1*) and the Δ*mppG* mutant (*lane 2*) with the primer pair of MppEup-F and MppEdw-R. The resulting PCR products were digested with *Nhe*I. Lane M indicates a DNA molecular weight marker, with sizes of 0.1, 0.2, 0.3, 0.4, 0.5, 0.6, 0.8, 1.0, 1.5, 2.0, 3.0, 4.0, 5.0, 6.0, 8.0 and 10.0 kb (from *bottom* to *top*). *Highlighted* with the *bars* are 1.0- and 3.0-kb fragments

of exogenous **Y-1**, 5 mg of **Y-1** was added to a 50-mL PDB culture of the Δ*MpPKS5* mutant at 3 days after the initiation of the culture [4]. After 4 days of incubation, the culture was harvested for extraction.

Gene inactivation

The primers used in this study are listed in Table 1. Polymerase chain reaction (PCR) was performed with Herculase II Fusion DNA Polymerase (Agilent, Santa Clara, CA, USA). To prepare the *mppG* inactivation construct, 1856- and 1819-bp DNA fragments upstream and downstream of *mppG* were PCR amplified with the primer pairs of MppGup-F/MppGup-R and MppGdw-F/MppGdw-R, respectively. These two fragments were cloned such that they flanked a 3.9-kb hygromycin resistance cassette (*hyg*) in pCAMBIA1300 (GenBank accession no. AF234296) through a three-fragment ligation using an In-Fusion cloning method (Clontech, Mountain View, CA, USA), generating pBIJ19 (Fig. 2B). A primer pair of hyg-F/hyg-mppG-R was used to amplify *hyg* from pUR5750, which is a pBIN19 derivative containing *hyg* from pAN7.1 [30]. The inactivation construct pBIJ19 was introduced into *M. purpureus* through an *Agrobacterium*-mediated transformation as previously described [31].

Table 1 Primers used in this study. The nucleotide sequences introduced for In-Fusion cloning are italicized and underlined

Name	Sequence (5′ → 3′)
MppGup-F	*CCATGATTACGAATTC*AAGGGGACGTTGATGTCTTG
MppGup-R	*GCTCGACGTATTTCA*ATAAGGACATCGCGGTTGAC
hyg-F	TGAAATACGTCGAGCCTGCT
hyg-mppG-R	*AGCCACCAGAAGACA*CCTGTGCATTCTGGGTAAAC
MppG-dw-F	TGTCTTCTGGTGGCTGTACG
MppG-dw-R	*TACCGAGCTCGAATTC*CGGACCATCATCTTCTTCGT

The sequence information was retrieved from the *M. purpureus* genome sequence portal of the Department of Energy-Joint Genome Institute

Chemical analysis methods

Thin-layer chromatography (TLC) was performed on silica gel 60 F_{254} TLC plates (Merck), which were developed with a mixture of n-hexane, ethyl acetate and formic acid (24:18:1). Ultraviolet (UV)–visible absorption spectra were collected with a Cary50 spectrophotometer (Varian, Palo Alto, CA, USA). HPLC analysis was performed on a ProStar system (Varian) with a Gemini C18 column (150 × 3.0 mm, 5.0 μm; Phenomenex, Torrance, CA,

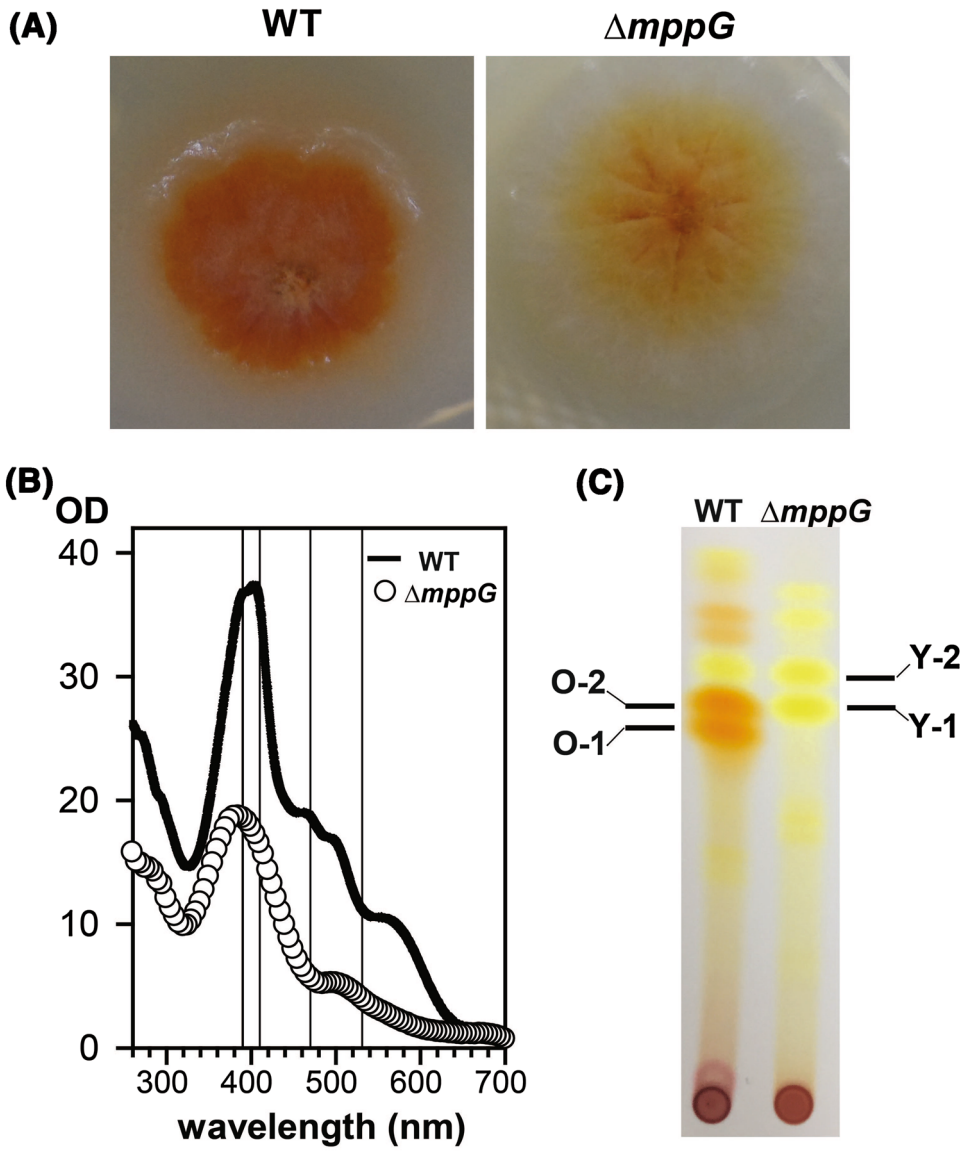

Fig. 3 The production of orange MAz was abolished in the Δ*mppG* mutant when cultured on PDA. (**A**) Approximately 3 cm^2 blocks of PDA cultures were placed on new PDA media and maintained for 5 days. (**B**) UV–visible spectra of the organic extracts were collected with proper dilutions in methanol, and the data were converted to the corresponding values in the original culture volume. These values are indicated as OD in the *y*-axis. The WT and Δ*mppG* strains are represented by a bold line and unfilled circles, respectively. The wavelengths characteristic of MAz is indicated as *Y*-axis reference lines at 390, 410, 470 and 530 nm. (**C**) TLC traces of the organic extracts on silica gel

USA), and the elution was monitored at 330 nm. The mobile phase consisted of 0.1% formic acid in water (A) and 0.1% formic acid in acetonitrile (B) [32]. The flow rate was maintained at 0.5 mL/min. The system was run with the following gradient program: 100% A for 5 min, from 100% A to 100% B over 20 min, then maintained at 100% B for 10 min. For the analysis of the PDB extracts, the gradient elution started from 50% A; after 5 min, the eluent composition was changed to 100% B over 20 min. For large-scale injections, a semi-preparative ODS-A C-18 column (250 × 10 mm, particle size of 5 µm, pore size of 12 nm; YMC, Kyoto, Japan) was used with a flow rate of 1.5 mL/min. The system was run with the following gradient program: 100% A for 5 min, from 100% A to 90% A over 25 min, from 90% A and 100% B over 20 min, then maintained at 100% B for 20 min.

Results and discussion

Targeted inactivation of *mppG* in *M. purpureus*

An *mppG* knockout mutant (Δ*mppG*) was generated by deleting a 951-bp internal region and replacing it with *hyg* (Fig. 2B). A PCR using the primer pair MppGup-F/MppGdw-R amplified ~5-kb-sized fragment from the wild-type (WT) DNA. The expected size for this WT fragment is 4.6 kb, and its identity was verified by a *Nhe*I digestion that generated expected fragments of 3.8 and 0.8 kb (Fig. 2C). The 4.6-kb WT band was absent in an identical PCR of the Δ*mppG* DNA, with ~8-kb-sized fragment being evident instead. The successful marker replacement in the chromosome was expected to yield a 7.7-kb band in this PCR amplification. This Δ*mppG* band was also subjected to a *Nhe*I digestion, which resulted in 4.1-, 2.6- and 0.8-kb-sized fragments, confirming the genotype of the Δ*mppG* strain (Fig. 2).

Dramatic reduction of orange MAz production in the Δ*mppG* strain

In a PDA culture, the Δ*mppG* mutant mycelia displayed a yellow hue and were easily distinguishable from the orange color of the WT strain (Fig. 3A). In UV–visible absorption measurements of the organic extracts, the Δ*mppG* mutant displayed an overall reduction in the visible absorption (Fig. 3B). It needs noting that the orange and red MAz compounds have considerable absorption near 400 nm, as well as at 470–530 nm. Thus, the visible absorption spectrum itself is incapable of deciphering the MAz profile in detail. In a TLC analysis of the extracts, there is evident dominance of orange MAz in the WT strain, and this orange MAz could not be found in the Δ*mppG* mutant (Fig. 3C). Yellow MAz **Y-1** and **Y-2** in the Δ*mppG* mutant appeared prominent due to the absence of orange MAz. **Y-1** and **O-2** overlapped in this TLC analysis, where the four MAz compounds were validated with the isolated compounds [28]. We need to mention that the TLC positions of

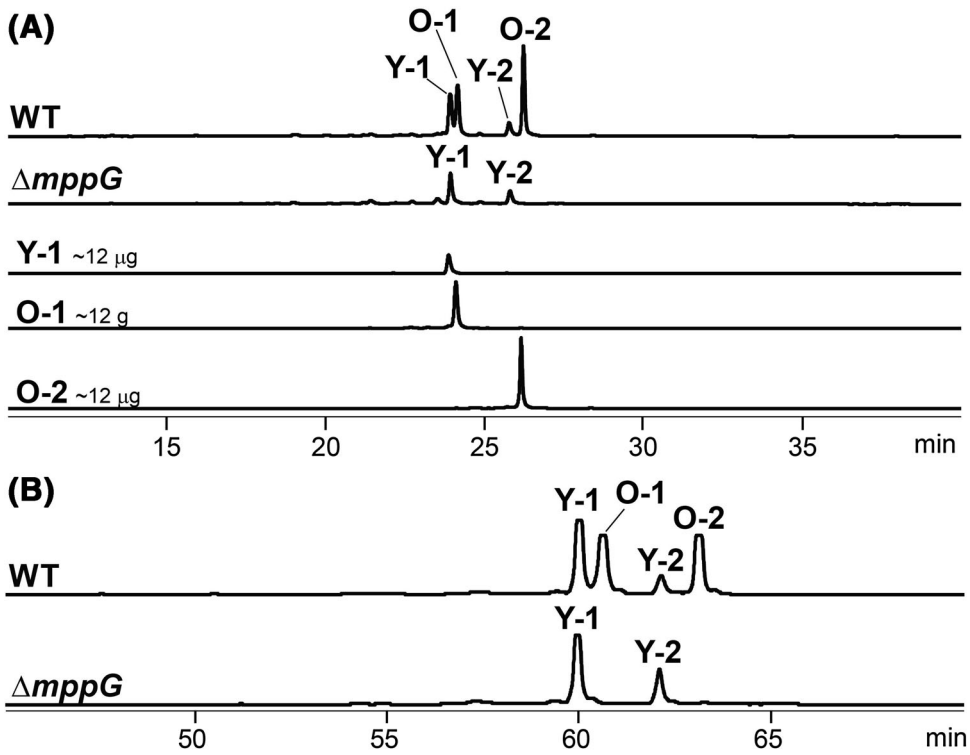

Fig. 4 HPLC analysis of the organic extracts from the PDA cultures of the WT and Δ*mppG* strains on analytical (**A**) and semi-preparative (**B**) reverse-phase columns. For analytical column analysis in (**A**), 2 µL of the samples was applied from 50 mL culture extracts dissolved in 1 mL methanol. HPLC traces were monitored at 330 nm and are drawn to the same scale

O-1 and **O-2** were mistakenly reversed in the previous report [28].

HPLC analyses also indicated that orange MAz compounds were absent in the Δ*mppG* mutant, while approximately 5 and 8 mg of **O-1** and **O-2**, respectively, were found in the WT strain (Fig. 4A). Notably, the level of **Y-1** was comparable between the WT and Δ*mppG* strain, and the content of **Y-1** was calculated to be approximately 6 mg from each 50 mL culture. Further analysis using a semi-preparative column also confirmed that yellow MAz compounds were absent in the Δ*mppG* mutant (Fig. 4B). This pattern was consistently observed in three independent trials. These experiments indicate that the biosynthesis of orange MAz involves *mppG*, and that the inactivation of *mppG* impaired orange MAz production, at least when grown on PDA plate.

We further investigated the MAz profile of the Δ*mppG* mutant in a PDB submerged culture. The visible spectra of the extracts showed a pattern similar to that of the PDA cultures, which was an overall reduction in the Δ*mppG* mutant (Fig. 5A). A TLC analysis of the WT extract indicated that orange MAz **O-1** and **O-2** were predominant and the yellow MAz bands were too faint to be reliably assigned (Fig. 5B). The production of orange MAz was

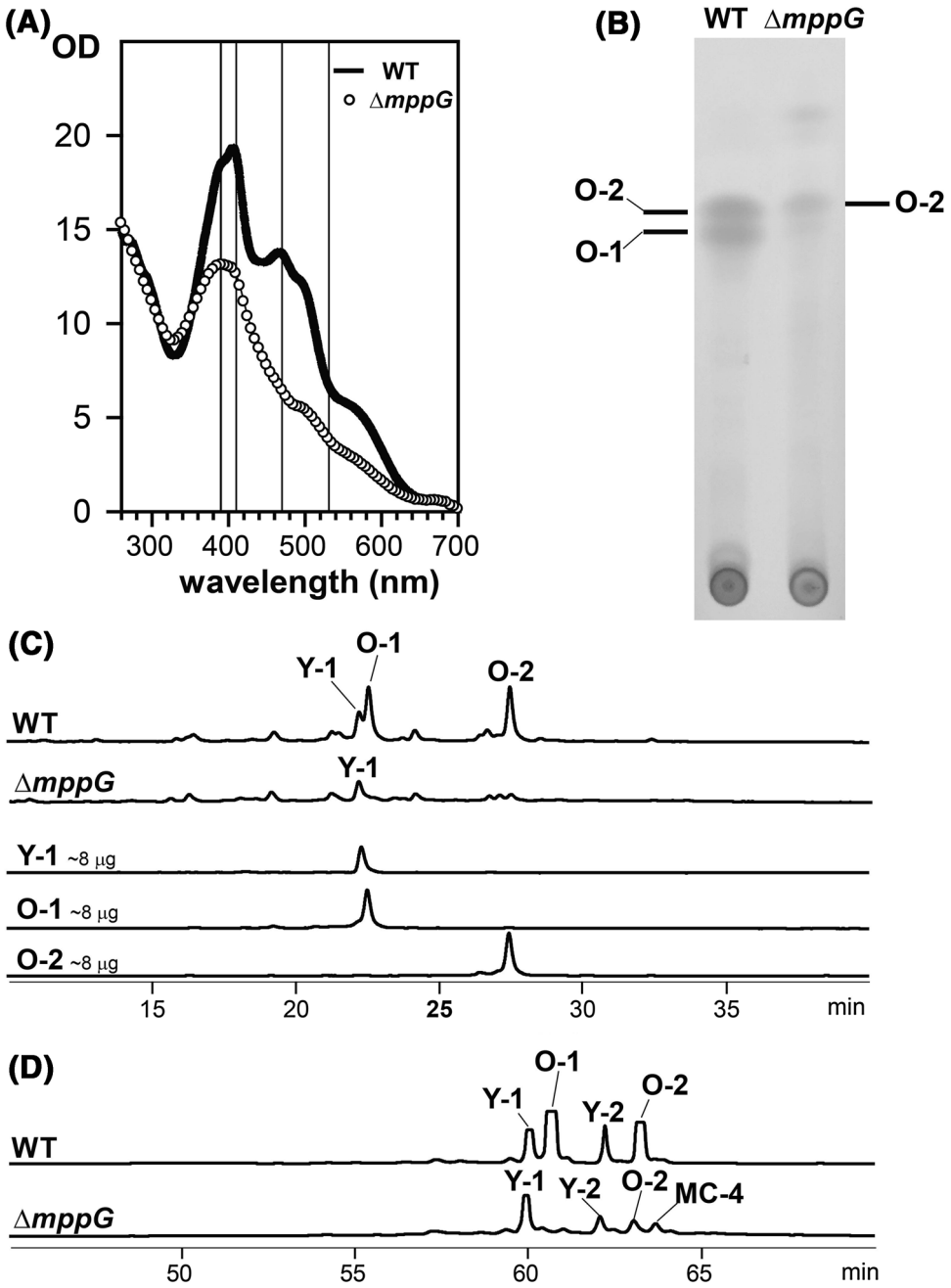

Fig. 5 The production of orange MAz was severely impaired in the Δ*mppG* mutant in the PDB submerged culture. (**A**) UV–visible spectra of the organic extracts that were collected with proper dilutions in methanol. The data were converted to represent the values in the original culture volume and are indicated as OD on the *y*-axis. The WT and Δ*mppG* strains are represented by a *bold line* and *unfilled circles*, respectively. The wavelengths characteristic of MAz is indicated as *Y*-axis reference lines at 390, 410, 470 and 530 nm. TLC (**B**) and HPLC (**C**, **D**) analyses of the WT and Δ*mppG* extracts. For HPLC analyses, both analytical (**C**) and semi-preparative (**D**) columns were used. For the analytical column analysis in (**C**), 2 μL of the samples was applied from 50 mL culture extracts dissolved in 1 mL methanol. HPLC traces that were monitored at 330 nm are drawn to the same scale

severely impaired in the Δ*mppG* mutant, although **O-2** was apparently present. The presence of **O-2** was a distinguishable feature in the PDB experiment when compared with the PDA experiment results in Figs. 3 and 4. HPLC analyses revealed several minor peaks in the PDB extracts, and thus, the HPLC gradient elution method was slightly modified to resolve peaks relevant to this experiment. This HPLC analysis verified a severe impairment in the production of orange MAz in the extract from the Δ*mppG* extract (Fig. 5C). An HPLC analysis on a semi-preparative column displayed two distinctive peaks near the elution time of **O-2** (Fig. 5D). These two peaks were collected from a repeat HPLC elution and were subjected to a ^{1}H-NMR measurement, which confirmed the identities of **O-2** and **MC-4** (data not shown). **MC-4** is a MAz derivative that accumulates in a Δ*mppC* mutant [25] and was isolated as a mixture with **O-2** in this experiment. **MC** stands for *mppC,* and the four MAz compounds from the Δ*mppC* mutant are designated **MC-1** to **-4** according to their elution order in a reverse-phase HPLC [25]. It better be noted that **MC-4** could be produced in WT at a trace level [25]. A residual production of **O-2** in the Δ*mppG* mutant implies that there exists another pathway that does not involve *mppG*, though the *mppG* pathway serves as the main pathway for orange MAz production. We also generated an *mppG* expression strain by introducing *mppG* under the control of *trpC* promoter in WT. This strain showed no significant difference from WT in the pigment production in several culture conditions tested (data not shown).

No conversion of Y-1 to O-1 occurred in a Δ*MpPKS5* mutant of *M. purpureus*

The MAz polyketide pathway produces two distinctive structural types of yellow MAz and orange MAz. It has been assumed that one group is the precursor to the other; orange MAz is converted into yellow MAz or vice versa. Bioorganic postulation based on an aromatic polyketide biosynthetic mechanism predicted that the MAz pathway generates orange MAz that is then reduced into yellow MAz [4]. The involvement of the pyranoquinone intermediate azanigerone E supports this idea (Fig. 1). Hypothesis that yellow MAz is converted into orange MAz has also been proposed. The continuous extraction of yellow MAz resulted in its selective production over orange MAz [20]. Based on this observation, the authors suggested that yellow MAz serves as a precursor for orange MAz, and that the extraction of yellow MAz into the culture medium limits the production of orange MAz. A biochemical mechanism for this proposal was not detailed, however.

The present experiments demonstrated that *mppG* is involved in orange MAz biosynthesis. We propose that *mppG* is specifically involved in orange MAz production but not in yellow MAz. This proposal is based on a divergent pathway hypothesis (Fig. 1). However, we could not exclude the possibility that **Y-1** (or **Y-2**) was converted into **O-1** (or **O-2**) by the oxidase MppG, and this step is blocked in the Δ*mppG* mutant. To clarify this issue, we performed a bioconversion experiment of **Y-1** in *M. purpureus* by supplying **Y-1** in a PDB submerged culture of

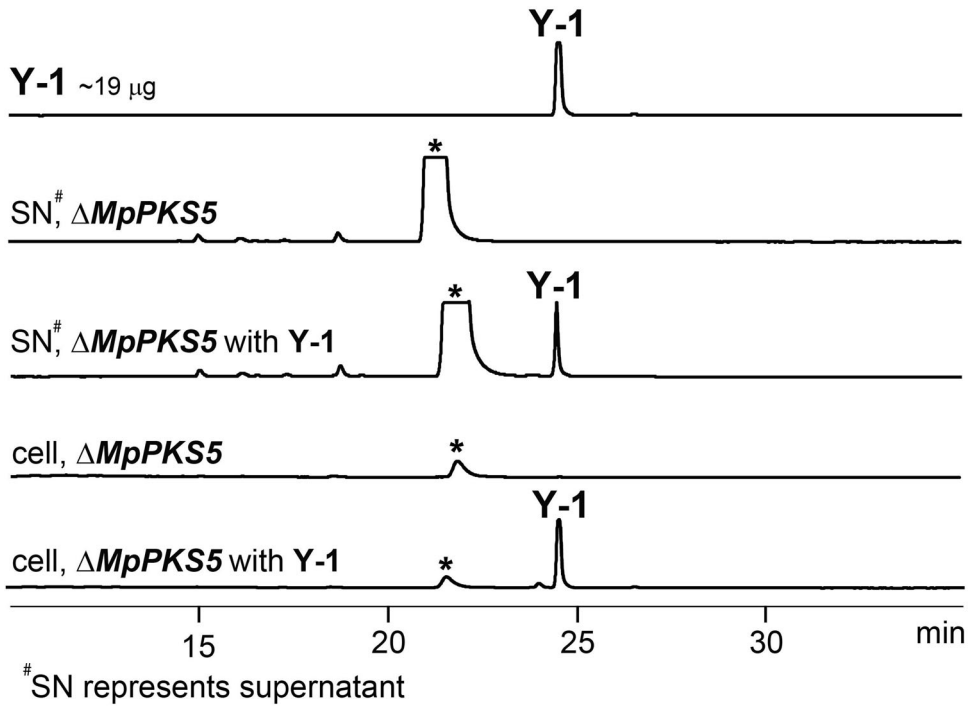

Fig. 6 Addition of **Y-1** to the *M. purpureus* Δ*MpPKS5* PDB culture. SN denotes supernatant. Citrinin peaks are marked with asterisks. HPLC traces that were monitored at 330 nm are drawn to the same scale

Δ*MpPKS5* and then examining whether **O-1** is generated or not. The Δ*MpPKS5* mutant is deficient at the first stage of MAz biosynthesis and is incapable of producing any MAz compounds [4]. An HPLC analysis confirmed that a substantial amount of **Y-1** was recovered from the cells, indicating that **Y-1** can be taken in by *M. purpureus* cells (Fig. 6). A high production of citrinin is a characteristic feature of the Δ*MpPKS5* mutant, with citrinin generally being found in the culture supernatant. **O-1** was not found in the extract, indicating that the Δ*MpPKS5* strain is incapable of converting **Y-1** into **O-1**. We therefore conclude that there is no biochemical activity that converts **Y-1** into **O-1** in *M. purpureus* and that *mppG* is specifically involved in orange MAz biosynthesis.

This study is the first report to describe the genetic factor that selectively contributes to the biosynthesis of orange MAz in *Monascus*. A characteristic feature of the Δ*mppG* mutant strain is a loss in the productivity of orange MAz, with no significant change in the production of yellow MAZ. This metabolic feature could provide an advantage in the preparation of yellow MAZ from *Monascus* products, and MppG is proposed to be the oxidase that completes orange MAz biosynthesis.

Acknowledgment This research was supported by Basic Science Research Program through the National Research Foundation of Korea (NRF) funded by the Ministry of Education (NRF-2016R1D1A1B02009237).

References

1. Gao JM, Yang SX, Qin JC (2013) Azaphilones: chemistry and biology. Chem Rev 113:4755–4811
2. Feng Y, Shao Y, Chen F (2012) *Monascus* pigments. Appl Microbiol Biotechnol 96:1421–1440
3. Patakova P (2013) *Monascus* secondary metabolites: production and biological activity. J Ind Microbiol Biotechnol 40:169–181
4. Balakrishnan B, Karki S, Chiu SH, Kim HJ, Suh JW, Nam B, Yoon YM, Chen CC, Kwon HJ (2013) Genetic localization and in vivo characterization of a *Monascus* azaphilone pigment biosynthetic gene cluster. Appl Microbiol Biotechnol 97:6337–6345
5. Shi K, Chen G, Pistolozzi M, Xia F, Wu Z (2016) Improved analysis of *Monascus* pigments based on their pH-sensitive UV–Vis absorption and reactivity properties. Food Addit Contam Part A Chem Anal Control Expo Risk Assess 33:1396–1401
6. Jung H, Kim C, Kim K, Shin CS (2003) Color characteristics of *Monascus* pigments derived by fermentation with various amino acids. J Agric Food Chem 51:1302–1306
7. Mapari SA, Thrane U, Meyer AS (2010) Fungal polyketide azaphilone pigments as future natural food colorants? Trends Biotechnol 28:300–307
8. Manzoni M, Rollini M (2002) Biosynthesis and biotechnological production of statins by filamentous fungi and application of these cholesterol-lowering drugs. Appl Microbiol Biotechnol 58:555–564
9. Lee CL, Pan TM (2012) Development of *Monascus* fermentation technology for high hypolipidemic effect. Appl Microbiol Biotechnol 94:1449–1459
10. Lee CL, Kung YH, Wu CL, Hsu YW, Pan TM (2010) Monascin and ankaflavin act as novel hypolipidemic and high-density lipoprotein cholesterol-raising agents in red mold dioscorea. J Agric Food Chem 58:9013–9019
11. Lee CL, Wen JY, Hsu YW, Hsu YW, Pan TM (2016) The blood lipid regulation of *Monascus*-produced monascin and ankaflavin via the suppression of low-density lipoprotein cholesterol assembly and stimulation of apolipoprotein A1 expression in the liver. J Microbiol Immunol Infect. doi:10.1016/j.jmii.2016.06.003
12. Lee CL, Hung YP, Hsu YW, Pan TM (2013) Monascin and ankaflavin have more anti-atherosclerosis effect and less side effect involving increasing creatinine phosphokinase activity than monacolin K under the same dosages. J Agric Food Chem 61:143–150
13. Hsu WH, Pan TM (2014) Treatment of metabolic syndrome with ankaflavin, a secondary metabolite isolated from the edible fungus *Monascus* spp. Appl Microbiol Biotechnol 98:4853–4863
14. Hsu WH, Pan TM (2014) A novel PPARgamma agonist monascin's potential application in diabetes prevention. Food Funct 5:1334–1340
15. Hsu LC, Liang YH, Hsu YW, Kuo YH, Pan TM (2013) Anti-inflammatory properties of yellow and orange pigments from *Monascus purpureus* NTU 568. J Agric Food Chem 61:2796–2802
16. Chang YY, Hsu WH, Pan TM (2015) *Monascus* secondary metabolites monascin and ankaflavin inhibit activation of RBL-2H3 cells. J Agric Food Chem 63:192–199
17. Lee CL, Wen JY, Hsu YW, Pan TM (2013) *Monascus*-fermented yellow pigments monascin and ankaflavin showed antiobesity effect via the suppression of differentiation and lipogenesis in obese rats fed a high-fat diet. J Agric Food Chem 61:1493–1500
18. Shi YC, Pan TM (2011) Beneficial effects of *Monascus purpureus* NTU 568-fermented products: a review. Appl Microbiol Biotechnol 90:1207–1217
19. Shi K, Song D, Chen G, Pistolozzi M, Wu Z, Quan L (2015) Controlling composition and color characteristics of *Monascus* pigments by pH and nitrogen sources in submerged fermentation. J Biosci Bioeng 120:145–154
20. Xiong X, Zhang X, Wu Z, Wang Z (2015) Accumulation of yellow *Monascus* pigments by extractive fermentation in non-ionic surfactant micelle aqueous solution. Appl Microbiol Biotechnol 99:1173–1180
21. Hu M, Zhang X, Wang Z (2016) Releasing intracellular product to prepare whole cell biocatalyst for biosynthesis of *Monascus* pigments in water–edible oil two-phase system. Bioprocess Biosyst Eng 39:1785–1791
22. Mo SJ, Suh JW (2016) Elucidation of first step of the allyl-malonyl-CoA biosynthetic pathway by expression of heterologous KSIII gene and enhancement of 36-methyl-FK506 production by genetic and chemical engineering. Appl Biol Chem 59:77–88
23. Joo M, Yoo HG, Kim HJ, Kwon HJ (2015) ToxB encodes a canonical GTP cyclohydrolase II in toxoflavin biosynthesis and *ribA* expression restored toxoflavin production in a Δ*toxB* mutant. J Korean Soc Appl Biol Chem 58:877–885
24. Balakrishnan B, Chen CC, Pan TM, Kwon HJ (2014) Mpp7 controls regioselective Knoevenagel condensation during the biosynthesis of *Monascus* azaphilone pigments. Tetrahedron Lett 55:1640–1643
25. Bijinu B, Suh JW, Park SH, Kwon HJ (2014) Delineating *Monascus* azaphilone pigment biosynthesis: oxidoreductive modifications determine the ring cyclization pattern in azaphilone biosynthesis. RSC Adv 4:59405–59408
26. Zabala AO, Xu W, Chooi YH, Tang Y (2012) Characterization of a silent azaphilone gene cluster from *Aspergillus niger* ATCC

1015 reveals a hydroxylation-mediated pyran-ring formation. Chem Biol 19:1049–1059
27. Balakrishnan B, Kim HJ, Suh JW, Chen CC, Liu KH, Park SH, Kwon HJ (2014) *Monascus* azaphilone pigment biosynthesis employs a dedicated fatty acid synthase for short chain fatty acyl moieties. J Korean Soc Appl Biol Chem 57:191–196
28. Balakrishnan B, Park SH, Kwon HJ (2017) A reductase gene *mppE* controls yellow component production in azaphilone polyketide pathway of *Monascus*. Biotechnol Lett 39:163–169
29. Chen C, Wang Y, Su C, Zhao XQ, Li M, Meng XW, Jin YY, Yang SH, Ma YS, Wei DZ, Suh JW (2015) Antifungal activity of *Streptomyces albidoflavus* L131 against the leaf mold pathogen *Passalora fulva* involves membrane leakage and oxidative damage. J Korean Soc Appl Biol Chem 58:111–119
30. de Groot MJ, Bundock P, Hooykaas PJ, Beijersbergen AG (1998) *Agrobacterium tumefaciens*-mediated transformation of filamentous fungi. Nat Biotechnol 16:839–842
31. Michielse CB, Hooykaas PJ, van den Hondel CA, Ram AF (2008) *Agrobacterium*-mediated transformation of the filamentous fungus *Aspergillus awamori*. Nat Protoc 3:1671–1678
32. Lee H, Kim E, Shin Y, Lee JH, Hur HG, Kim JH (2016) Identification and formation pattern of metabolites of cyazofamid by soil fungus *Cunninghamella elegans*. Appl Biol Chem 59:9–14